23rd ABCM International Congress of Mechanical Engineering
December 6-11, 2015, Rio de Janeiro, RJ, Brazil

NUMERICAL ANALYSIS OF THE HEAT TRANSFER IN THE EXHAUST PIPE OF A DIESEL POWER GENERATOR

Cristiano Henrique Gonçalves de Brito
José Ricardo Sodré
Cristiana Brasil Maia
Pontifícia Universidade Católica de Minas Gerais – Dom José Gaspar, 500, Belo Horizonte/MG - Brazil
cristianohbrito@globo.com, ricardo@pucminas.br, cristiana@pucminas.br

Abstract. *This paper presents a numerical study of the heat transfer in the exhaust pipe of a diesel power generator to determine the exhaust gas temperature profiles. The numerical simulations were performed for the engine operating under the loads of 0, 10, 20 and 40 kW. The Ansys CFX software was used to solve the conservation and transport equations of the turbulent fluid flow. The k-omega SST turbulence model was used, along with literature correlations for the convection heat transfer coefficients. The numerical results for heat transfer in exhaust gas were compared with literature data. The results revealed that the temperature gradient increased with increasing load applied to the engine, causing enlargement of the temperature profiles due to increased temperature and reduced mass flow rate of the exhaust gas. It was also found that the temperature profiles are significantly altered by recirculation of fluid flow caused by adverse pressure gradients. The results showed good agreement with literature data.*
Keywords: *Numerical simulation, Exhaust gas temperature, Diesel engine, Energy, CFD*

1. INTRODUCTION

Due to recent climate changes and human actions that accelerate and enhance these changes and the possible scarcity of fossil fuels, every year increases the need to develop more efficient and less polluting engines (Drenth et al., 2014). In this scenario, the research in internal combustion engines have given special focus to exhaust systems. Quantitative information on the heat transfer in the exhaust system are important both for engine design as for predict the efforts to which the engine will be subjected (Caton and Heywood, 1981). Furthermore, the precise knowledge of the gas temperature is useful in determining suitable location devices such as catalysts, turbochargers or thermal electric generator. Studies verified that heat transfer in the exhaust gases substantially affects the catalyst functioning. Kandylas and Stamatelos (1999) concluded that the heat transfer in the exhaust system could be addressed as a solution of passive heating of the catalyst allowing a low level of emissions in the cold start of spark ignition engines. According to Gasser and Rybick (2013) the temperature is the fundamental parameter to control the efficiency of the catalyst and therefore the catalyst must be provided with a sufficiently high temperature for a short time after starting the engine. Models can be used to simulate the condition of gases, particularly regarding its behavior with temperature.

For Kesgin (2005), since usually the exhaust system does not present high temperatures and very complex gas flow phenomena, transfer rates and pressure losses can be optimized to improve engine performance and reduce the power loss by the exhaust system. Rakopoulos, Andritsakis and Hountalas (1995) used the finite difference method (FDM) to study heat transfer and fluid dynamics of the exhaust gases flow in internal combustion engines. The authors verified the availability of energy contained in the gas and its influence on the performance of a diesel engine. Rakopoulos, Kosmadakis and Pariotis (2010) used a CFD (Computational Fluid Dynamics) commercial software to the more generic formulation of heat transfer problem in internal combustion engines, in order to obtain a method able to predict the mechanism heat transfer of engines in different configurations. The heat transfer in exhaust systems is directly related to the gases emissions and to the thermal efficiency of a combustion engine. Aware of this problem, Sekavcnik et al. (2012) used a commercial CFD software to evaluate the exergy destruction in the engine, and found that 25% of the engine exergy is destroyed in the flow of exhaust gases. Because of the importance of determining the temperature profiles in the exhaust duct, Brito, Andrade and Sodré (2014) used the MDF techniques to solve the energy equation in the flow of exhaust gases, modeling the exhaust gases as air with constant properties and considering laminar and fully developed flow. Subsequently, Brito, Maia and Sodré (2014) improved the model to solve the energy equation proposing a turbulent profile for the velocity and air properties varying with temperature.

The main objective of this paper is to study the behavior of the exhaust gases of a diesel power generator using CFD techniques. The commercial software Ansys CFX ® was used to solve the governing equations of the turbulent flow. The simulation was performed considering the exhaust gases as a combination of six species of combustion products, for engine operation under loads from 0 to 40 kW.

2. PROBLEM FORMULATION

The exhaust system is one of the main engine power sinks, where about 30% of energy from combustion is lost (Pulkabrek, 1997). The heat loss through the exhaust system affects the engine efficiency and the emission levels. The determination of the heat lost could help to improve the thermal efficiency, through the use of energy recovery devices, and to optimize the catalytic converter and devices, reducing engine emission levels. The energy carried by the exhaust gases can be evaluated from the analysis of the internal fluid flow.

In this paper, it was simulated an exhaust pipe of a diesel engine. The geometric parameters used in the analysis were obtained from an experimental prototype, shown in Fig. 1a. The computational domain and exhaust pipe dimensions are shown in Fig. 1b and Fig. 1c, respectively.

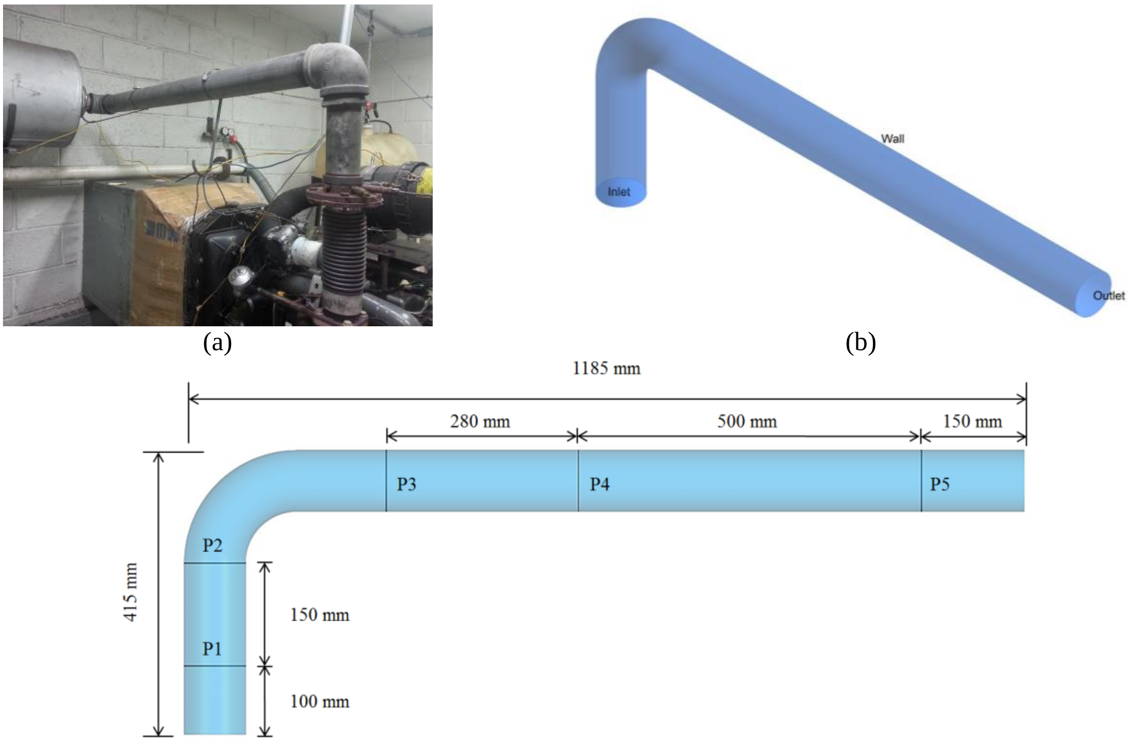

(c)

Figure 1. Exhaust pipe: (a) physical domain, (b) computational domain and (c) exhaust pipe dimensions

2.1 Governing equations

The equations governing the fluid flow are the mass, momentum and the energy conservation equations (Minkowycz; Sparrow and Murthy, 2006), and the transport equations for the turbulent properties:

- Mass conservation equation (White, 2006):

$$\frac{\partial}{\partial t}\rho+\nabla\bullet\left(\rho\overline{\mathbf{U}}\right)=0 \tag{1}$$

- Momentum conservation equation (White, 2006):

$$\frac{D\left(\rho\overline{\mathbf{U}}\right)}{Dt}=\rho\mathbf{g}-\nabla\overline{p}+\nabla\bullet\tau_{ij} \tag{2}$$

Where stress tensor is given by (White, 2006):

$$\tau_{ij}=\mu\left(\frac{\partial u_i}{\partial x_j}+\frac{\partial u_j}{\partial x_i}\right)-\rho\overline{u_i'u_j'} \tag{3}$$

- Energy conservation equation (White, 2006):

$$\rho c_p \frac{D\overline{T}}{Dt} = -\frac{\partial}{\partial x_i} q_i + \overline{\Phi} \tag{4}$$

Where heat flux is given by (White, 2006):

$$q_i = -k\frac{\partial \overline{T}}{\partial x_i} + \rho c_p \overline{u_i' T'} \tag{5}$$

And the viscous dissipation function is (White, 2006):

$$\overline{\Phi} = \overline{\frac{\mu}{2}\left(\frac{\partial \overline{u}_i}{\partial x_j} + \frac{\partial u_i'}{\partial x_j} + \frac{\partial \overline{u}_j}{\partial x_i} + \frac{\partial u_j'}{\partial x_i}\right)^2} \tag{6}$$

The *K*-ω SST model was used to evaluate the turbulent properties (Veersteg and Malalasekera, 2007). For the turbulent kinetic energy (*K*):

$$\frac{\partial(\rho K)}{\partial t} + \nabla \bullet (\rho K \mathbf{U}) = \nabla \bullet \left[\left(\mu + \frac{\mu_t}{\sigma_K}\right)\cdot \nabla(K)\right] + \left(2\rho S_{ij}\cdot S_{ij} - \frac{2}{3}\rho K \frac{\partial U_i}{\partial x_j}\delta_{ij}\right) - \mathcal{B}^* \rho K \omega \tag{7}$$

For the turbulent frequency (ω):

$$\frac{\partial(\rho \omega)}{\partial t} + \nabla \bullet (\rho \omega \mathbf{U}) = \nabla \bullet \left[\left(\mu + \frac{\mu_t}{\sigma_{\omega,1}}\right)\cdot \nabla(\omega)\right] + \gamma_2\left(2\rho S_{ij}\cdot S_{ij} - \frac{2}{3}\rho \omega \frac{\partial U_i}{\partial x_j}\delta_{ij}\right) - \mathcal{B}_2 \rho \omega^2 + 2\frac{\rho}{\sigma_{\omega,2}\cdot \omega}\frac{\partial K}{\partial x_K}\frac{\partial \omega}{\partial x_K} \tag{8}$$

The constants $\sigma_K = 1{,}0$, $\sigma_{\omega,1} = 2{,}0$, $\sigma_{\omega,2} = 1{,}17$, $\gamma_2 = 0{,}44$, and $\mathcal{B}_2 = 0{,}083$ are defined empirically.

2.2 Calculation of exhaust gas composition

The determining of exhaust gas composition can be made concerning chemical equilibrium composition and complete diesel combustion. The diesel products combustion involve more 232 species, among them those with higher concentration and that can be used in fluid flow along the exhaust pipe are: (1) CO_2; (2) H_2O; (3) N_2; (4) O_2; (5) CO_2; and (6) H_2; (Rakopoulos et al., 1994). The stoichiometric complete combustion reaction of hydrocarbon fuel is (Heywood, 1988)

$$C_n H_m O_r + \left(n + \frac{m}{4} - \frac{r}{2}\right)\cdot(O_2 + 3{,}773 N_2) = n_p(x_1 CO_2 . + x_2 H_2 O + x_3 N_2 + x_4 O_2 + x_5 CO + x_6 H_2) \tag{9}$$

Where x_i mole fraction of the *i* th component and n_p is mole number of products. For the diesel fuel modeled as docecano, n, m and r assumes the values 12, 26 and 0, respectively.

To solve the seven unknowns used, additional equations, the five balanced equations of carbon (Eq. 11), hydrogen (Eq. 12), oxygen (Eq. 13), nitrogen (Eq. 14) and mole fraction sum, assist in solving this problem.

$$n = n_p(x_1 + x_5) \tag{10}$$

$$m = n_p(2x_2 + 2x_6) \tag{11}$$

$$\left(n + \frac{m}{4} - \frac{r}{2}\right) = n_p(2x_1 + x_2 + 2x_4 + x_5) \tag{12}$$

$$7.546\left(n + \frac{m}{4} - \frac{r}{2}\right) = n_p(2x_3) \tag{13}$$

$$x_1 + x_2 + x_3 + x_4 + x_5 + x_6 = 1 \tag{14}$$

And the chemical equilibrium constant K_p, equations in Eq. (16) and Eq. (15), defined as a function of temperature, complete the seven equations needed for solve the mole fractions (Ferguson and Kirkpatrick, 2001).

$$CO_2 + H_2 \leftrightarrow CO + H_2O \tag{15a}$$

$$K_{p1} = \frac{x_1 x_6}{x_2 x_5} \tag{15b}$$

$$\ln(K_{p1}) = 2.743 - \frac{1.761}{(T/1000)} - \frac{1.611}{(T/1000)^2} + \frac{0.2803}{(T/1000)^3} \tag{15c}$$

$$CO + \frac{1}{2}O_2 \leftrightarrow CO_2 \tag{16a}$$

$$K_{p2} = \frac{x_1}{x_5\sqrt{x_4}} \tag{16b}$$

$$\log(K_{p2}) = -0.415302\ln\left(\frac{T}{1000}\right) - \frac{0.148627E5}{T} - 0.475746E1 + 0.124699E-3\cdot T - 0.900227E-8\cdot T^2 \tag{16c}$$

3. NUMERICAL METHODOLOGY

The governing equations were solved using the commercial software Ansys CFX® 14.5. The computational domain was the pipe geometry showed in Fig. 1b, considering 3-D steady state fluid flow.

The fundamental hypotheses adopted are:

- Exhaust gas with six species;
- Incompressible flow;
- Turbulent flow;
- Turbulence model: K-ω SST;

The boundary conditions adopted are:

- In the outlet, relative static pressure of 0 Pa;
- Conditions for non-slip walls;
- Constant mass flow rate at the inlet, given by experimental data;
- Constant temperature at the inlet, given by experimental data;
- Prescribed heat transfer coefficient in the duct walls;
- Ambient temperature of 27°C;

Experimental data from literature (Morais et al.. 2013) used in the numerical simulations are described in Table 1, collected with the diesel engine-generator set operating under loads of 0, 10, 20 and 40 kW.

Table 1. Entry conditions used in numerical simulations

Measured variable	**Size unit**	**Values obtained**			
Nominal power	kW	0	10	20	40
Ambient temperature	°C	27	27	27	27
Inlet temperature of exhaust gas	°C	149,4	239,4	332,1	598,3
Mass flow of exhaust gas	kg/h	148,4	144,7	142,7	133,0

A mesh test was carried out, starting from a coarse mesh and reducing the element size by a constant factor. The mesh tests and numerical simulation was performed for different engine operating loads.

4. RESULTS AND DISCUSSION

Using the conditions previously stated, a mesh test was carried out, starting from a coarse mesh and reducing the element size by a constant factor. The mesh tests and numerical simulation were performed for different engine operating loads. The reference point to evaluate the problem convergence was the point located 150 mm from the exit and 0.1 mm from the wall. Table 2 shows the test performed at 0 kW load, and Figure 2 shows the final mesh for this situation.

Table 2. Mesh tests results

RMS	MESH	ELEMENTS	NODES	TEMPERATURE [K]	VELOCITY [m/s]
10^{-6}	1	772200	789633	401,20	8,27
	2	519491	531960	401,19	8,26
	3	217022	223110	401,17	8,24
	4	169488	174125	400,92	8,24
10^{-5}	1	772200	789633	401,20	8,27
	2	519491	531960	401,19	8,26
	3	217022	223110	401,16	8,24
	4	169488	174125	400,92	8,24

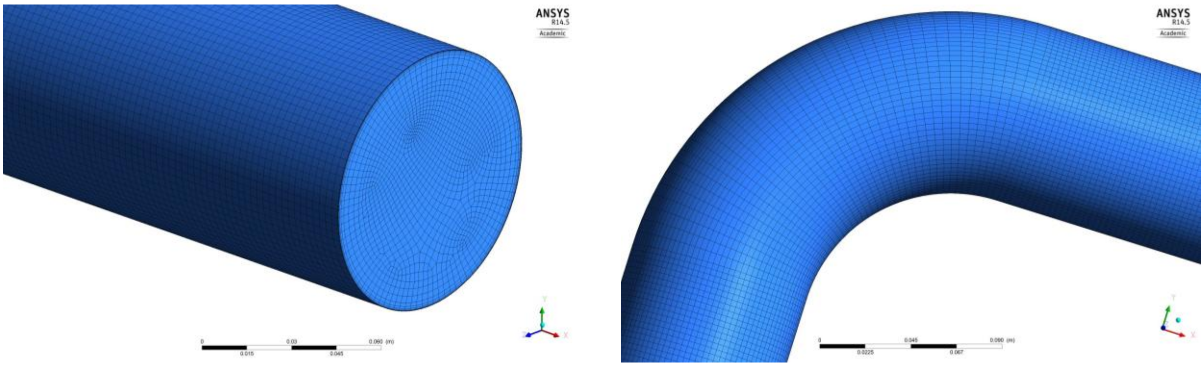

Figure 2. Mesh

Mesh 1 was defined as the mesh to be used in the simulations, using the proposed criterion. The simulation required 14 h 23 minutes to be concluded. The velocity profiles obtained for different engine operating loads are shown in Fig. 3.

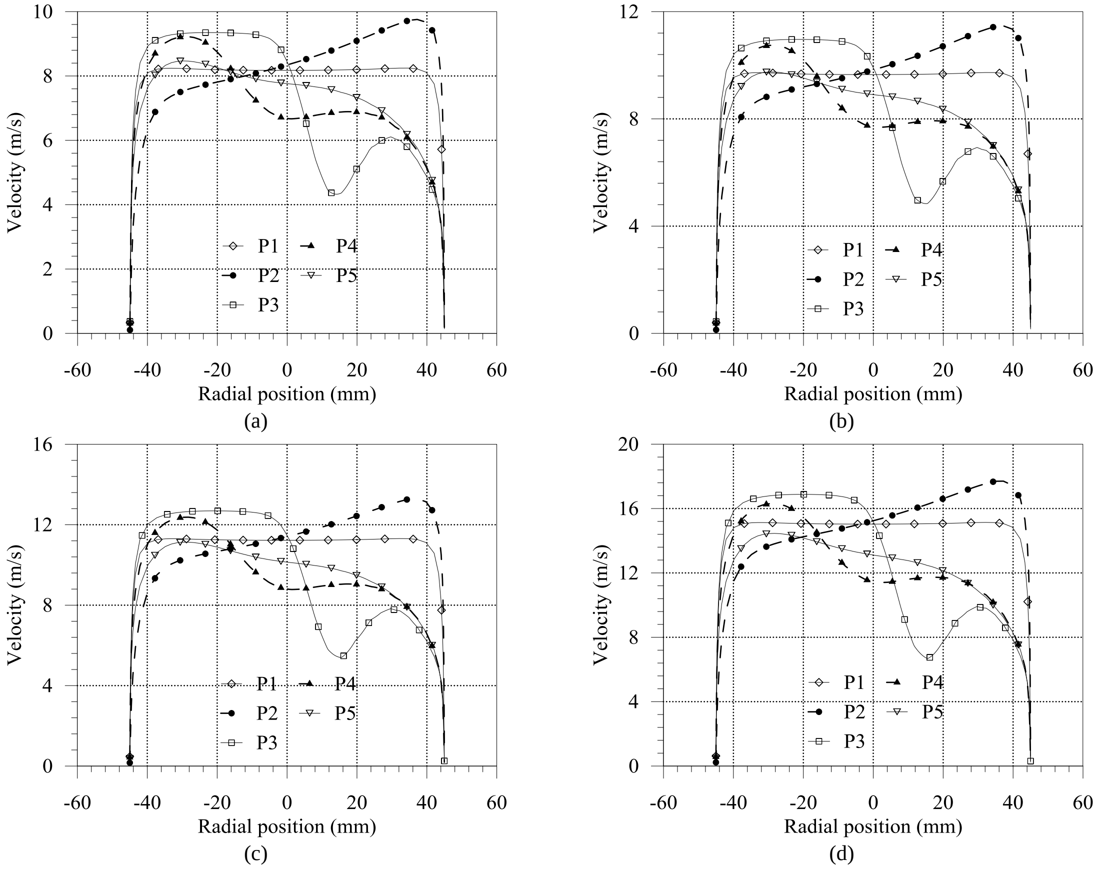

Figure 3. Velocity profiles for engine loads: (a) 0, (b) 10, (c) 20 and (d) 40 Kw

It can be seen that the general form of the velocity profiles of the behavior remained unchanged with the increasing engine load, even with a reduction on the mass flow rate. As shown in Fig. 3, the non-uniformity of velocity profiles along the axial direction indicates that the fluid flow is not fully developed, expected behavior due to the change of direction imposed by the duct curve. This changing of direction of the fluid flow promotes an adverse pressure gradient and a consequent detachment of the fluid recirculation right after the curve, as shown in Fig. 4a.

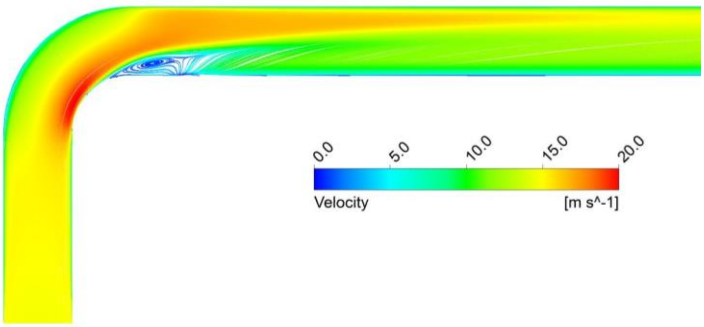

(a)

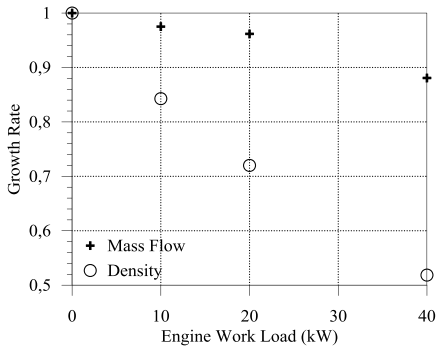

(b)

Figure 4. (a) Streamline of velocity for engine load operating 40 kW and (b) Growth rate of mass flow and density for different engine operating load

The average velocity increases with the load, in spite of the reduction of mass flow rate (Table 1). This behavior can be explained by the reduction of the average density, significantly greater than the reduction of the mass flow rate, as can be seen in Fig. 4b.

The temperature profiles obtained are shown in the Fig. 5. It is possible to verify that, with the increase of the load and a consequent increase in inlet temperature of the exhaust gases, the average temperature also increases.

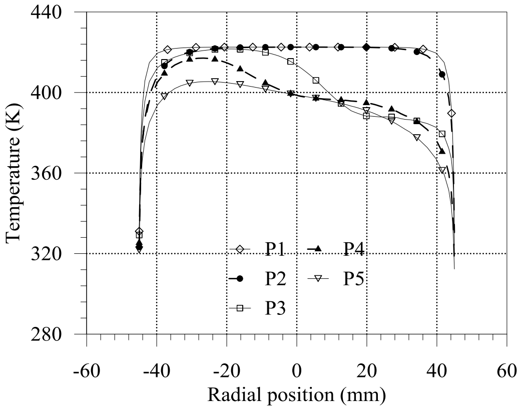

(a)

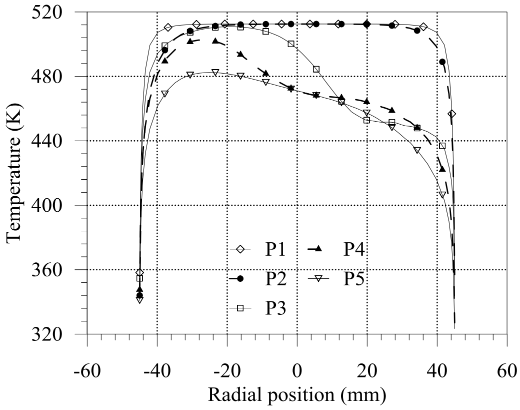

(b)

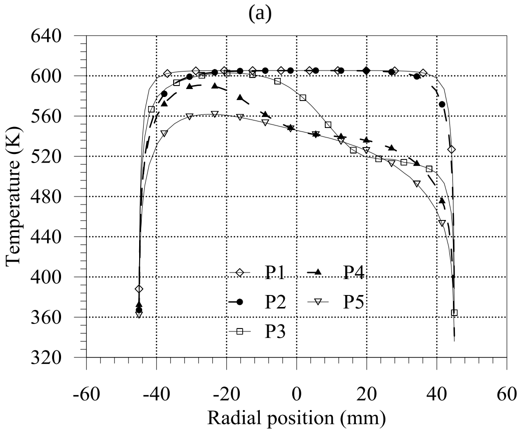

(c)

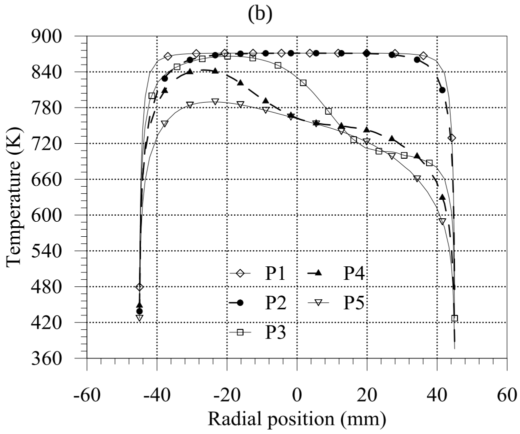

(d)

Figure 5. Temperature profiles for engine loads: (a) 0, (b) 10, (c) 20 and (d) 40 kW

It can be seen that the profile of temperature before the curve (points P1 and P2) is more uniform than after the curve (points P3, P4 and P5). This behavior is explained by the recirculation and detachment of the fluid next to the curve. Figure 6 presents the temperature field on the domain, showing the influence of these effects on the temperature.

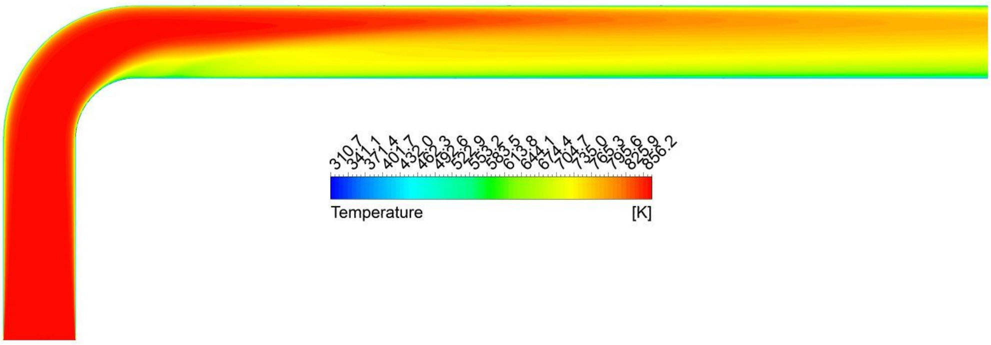

Figure 6. Temperature field for engine load operating 40 kW

Figure 7 shows the evolution of velocity profiles, temperature and density with engine load increases. As discussed, the average values of velocity and temperature increase with the load, and the density decreases with the load.

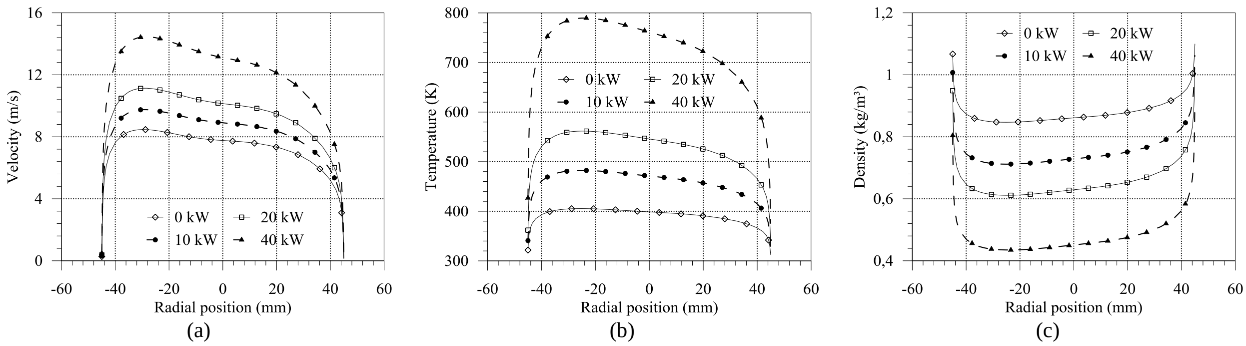

Figure 7. Changes in (a) velocity profile, (b) temperature and (c) density with increasing engine load

5. CONCLUSIONS

In this paper it was performed a numerical analysis of the exhaust gas of a diesel power generator. Ansys CFX® was used to solve the conservation equations of mass, momentum and energy, and the transport equations for the turbulent properties. The temperature and velocity profiles were obtained in the exhaust pipe of the engine, for different loads (0, 10, 20 and 40 kW).

Experimental data were used as inlet boundary condition. As the load increases, the mass flow rate decreased. However, the average velocities also increased, due to a great reduction observed on the density. The general form of the velocity profile, nevertheless, did not significantly change with the load. The average temperatures increased with the load, due to an increase on the inlet temperature observed experimentally. It was also observed that the temperature profiles are strongly influenced by the curve imposed on the pipe, since the heat transfer is maximized in this region leading to higher temperature gradients.

6. ACKNOWLEDGEMENTS

The authors gratefully acknowledge PUC-MG, CAPES, CNPq and FAPEMIG.

7. REFERENCES

ANSYS CFX. *CFX Solver Theory Manual.* Version 14.5, Ansys, 2013

Brito, C. H. G., Andrade, G. F., Sodré, J. R., 2014. “Análise do Perfil de Temperaturas no Duto de Exaustão de um Motor pelo Método das Diferenças Finitas”. In *Proceeding Series of the Brazilian Society of Computational and Applied Mathematics – CMAC Sul 2014.* Curitiba, Brazil.

Brito, C. H. G., Maia, C. B., Sodré, J. R., 2014. “Análise do Perfil de Temperaturas no Duto de Exaustão de um Motor Diesel”. In *Proceedings of the XXXV Iberian Latin-American Congress on Computational Methods in Engineering*. Fortaleza, Brazil.

Caton, J., Heywood, J., 1981. “An experimental and analytical study of heat transfer in engine exhaust port”. *International Journal Heat and Mass Transfer*, Vol. 24, p 581-595.

Drenth, A.C., Olsen, D. B., Cabot, P. E., Johnson, J. J., 2014. “Compression ignition engine performance and emissions evaluation of industrial oilseed biofuel feedstock camelina, carinata and pennycress across three fuel pathways”. In *Fuel*, Vol. 36, p 975-984.

Ferguson, C. R., Kirkpatrick, A. T., 2001. *Internal Combustion Engines: Applied Thermoscienses*. 2nd Edition. John Wiley & Sons Inc, USA.

Gasser, I., Rybicki, M., 2013. “Modelling and simulation of gas dynamics in exhaust pipe”. *Applied Mathematical Modelling*, Vol. 37, p 2747-2764.

Heywood, J. B., 1988. *Internal Combustion Engine Fundamentals.* McGraw-Hill, USA.

Kandylas, I., Stamatelos, A., 1999. “Engine exhaust system design based on heat transfer computation”. *Energy Conversion & Management*, Vol. 40, p 1057-1072.

Kesgin, U., 2005. “Study on the design of inlet and exhaust system of a stationary internal combustion engine”. *Energy Conversion & Management*, Vol. 46, p 2258-2287.

Minkowycz, W. J., Sparrow, E. M., Murthy, J. Y., 2006. *Handbook of Numerical Heat Transfer*. John Wiley & Sons, Inc, USA.

Morais, A. et al., 2013. “Hydrogen impacts on performance and CO2 emissions from a diesel power generator”. *Internal Journal of Hydrogen Energy*, Vol. 38, p 6857-6864.

Pulkrabek, W. W., 1997. *Engineering Fundamentals of The Internal Combustion Engine*. Prentice Hall.

Rakopoulos, C., Andritsakis, E., Hountalas, D., 1995. “The influence of the exhaust system unsteady gas flow and insulation on the performance of turbocharged diesel engine”. *Heat Recovery Systems & CHP*, Vol. 15, p 51-72.

Rakopoulos, C., Hountalas, D. T., Tzanos, E. I., Taklis, G. N., 1994. “A fast algorithm for calculating the composition of diesel combustion products using 11 species chemical equilibrium scheme”. *Advances in Engineering Software*, Vol. 19, p 109-119.

Rakopoulos, C., Kosmadakis, G., Pariotis, E., 2010. “Critical evaluation of current heat transfer models used in CFD in-cylinder engine simulations and establishment of a comprehensive wall-fuction formulation”. *Applied Energy*, Vol 87, p 1612-1630

Sekavcnik, M., Ogoreve, T., Katrasnik, T., Rodman-Opresnik, S., 2012. “Three-dimensional approach to exhaust gas energy analysis”. *Heat and Mass Transfer*, Vol. 48, p 923-931.

Versteeg, H. K., Malalasekera, W., 2007. *An Introduction to Computational Fluid Dynamics: The finite volume method.* Pearson Education, 2nd edition.

White, F. M., 2006. *Viscous Fluid Flow.* McGraw-Hill, 2006.

8. RESPONSIBILITY NOTICE

The authors are the only responsible for the printed material included in this paper.